

Journal of Child Neurology

<http://jcn.sagepub.com/>

Perfusion Imaging of Focal Cortical Dysplasia Using Arterial Spin Labeling: Correlation With Histopathological Vascular Density

Pia Wintermark, Mirna Lechpammer, Simon K. Warfield, Bela Kosaras, Masanori Takeoka, Annapurna Poduri, Joseph R. Madsen, Ann M. Bergin, Stephen Whalen and Frances E. Jensen
J Child Neurol 2013 28: 1474 originally published online 21 May 2013
DOI: 10.1177/0883073813488666

The online version of this article can be found at:
<http://jcn.sagepub.com/content/28/11/1474>

Published by:



<http://www.sagepublications.com>

Additional services and information for *Journal of Child Neurology* can be found at:

Email Alerts: <http://jcn.sagepub.com/cgi/alerts>

Subscriptions: <http://jcn.sagepub.com/subscriptions>

Reprints: <http://www.sagepub.com/journalsReprints.nav>

Permissions: <http://www.sagepub.com/journalsPermissions.nav>

>> [Version of Record](#) - Oct 18, 2013

[OnlineFirst Version of Record](#) - May 21, 2013

[What is This?](#)

Perfusion Imaging of Focal Cortical Dysplasia Using Arterial Spin Labeling: Correlation With Histopathological Vascular Density

Journal of Child Neurology
28(11) 1474-1482
© The Author(s) 2013
Reprints and permission:
sagepub.com/journalsPermissions.nav
DOI: 10.1177/0883073813488666
jcn.sagepub.com


Pia Wintermark, MD^{1,2,3}, Mirna Lechpammer, MD, PhD^{4,5,6},
Simon K. Warfield, PhD³, Bela Kosaras, MD⁶, Masanori Takeoka, MD⁶,
Annapurna Poduri, MD⁶, Joseph R. Madsen, MD⁷, Ann M. Bergin, MD⁶,
Stephen Whalen, PhD³, and Frances E. Jensen, MD⁶

Abstract

Focal cortical dysplasia is the most common malformation of cortical development, causing intractable epilepsy. This study investigated the relationship between brain perfusion and microvessel density in 7 children with focal cortical dysplasia. The authors analyzed brain perfusion measurements obtained by magnetic resonance imaging of 2 of the children and the microvessel density of brain tissue specimens obtained by epilepsy surgery on all of the children. Brain perfusion was approximately 2 times higher in the area of focal cortical dysplasia compared to the contralateral side. The microvessel density was nearly double in the area of focal cortical dysplasia compared to the surrounding cortex that did not have morphological abnormalities. These findings suggest that hyperperfusion can be related to increased microvessel density in focal cortical dysplasia rather than only to seizures. Further investigations are needed to determine the relationship between brain perfusion, microvessel density, and seizure activity.

Keywords

arterial spin labeling, cerebral blood flow, focal cortical dysplasia, magnetic resonance imaging, brain perfusion

Submitted January 20, 2013. Accepted for publication April 7, 2013.

Focal cortical dysplasia is one of the most common malformations of cortical development, causing intractable epilepsy. Two classifications are classically used to describe them. The morphological Palmini classification distinguishes mild dysplasia/microdysgenesis from focal cortical dysplasia with further subtypes distinguished according to cytopathological findings.¹ The International League Against Epilepsy (ILAE) Task Force proposed a detailed 3-tiered clinicopathological classification system for focal cortical dysplasia to better characterize specific clinicopathological entities.² Although the precise timing of the development of focal cortical dysplasia during ontogenesis is unknown, focal cortical dysplasia is thought to result from abnormal neuronal migration during corticogenesis.

Focal cortical dysplasia is an important cause of pharmacoresistant epilepsy that frequently requires surgical treatment. Prior to surgery for intractable epileptic seizures, multimodal epilepsy imaging, including magnetic resonance imaging (MRI), single-photon emission computed tomography, and positron emission tomography, is currently used to delineate focal cortical dysplasia and other cortical development malformations. The hyperperfusion and hypoperfusion observed on single-photon emission

computed tomography and positron emission tomography have been previously correlated with the hypermetabolism or hypometabolism related to seizures and interictal states and have been used to locate the focus to be removed by surgery.

Some previous observations have shown that focal cortical dysplasia and other malformations of cortical development are

¹ Division of Newborn Medicine, Department of Pediatrics, Montreal Children's Hospital, McGill University, Montreal, QC, Canada

² Division of Newborn Medicine, Children's Hospital Boston, Boston, MA, USA

³ Department of Radiology, Children's Hospital Boston, Boston, MA, USA

⁴ Department of Pathology, University of California Davis Medical Center, Sacramento, CA, USA

⁵ Department of Pathology, Children's Hospital Boston, Boston, MA, USA

⁶ Department of Neurology, Children's Hospital Boston, Boston, MA, USA

⁷ Department of Neurosurgery, Children's Hospital Boston, Boston, MA, USA

Corresponding Author:

Pia Wintermark, MD, McGill University, Montreal Children's Hospital, Division of Newborn Medicine, 2300 Rue Tupper, C-920, Montreal, QC H3H 1P3, Canada.

Email: pia.wintermark@bluemail.ch

associated with cerebral vascular alterations, including anomalies of large blood vessels, and also alterations of the microvasculature that are not only a consequence of epileptic activity.³⁻⁶ These observations prompted the authors to test the hypothesis that the hyperperfusion observed in focal cortical dysplasia correlates to an altered microvasculature in the affected tissue, especially an increase in the number of small-caliber blood vessels, which can be a contributing factor to, rather than a consequence of, seizures. Thus, this pilot study was designed to investigate the relationship between blood flow measurements based on perfusion imaging by arterial spin labeling and the associated histopathological findings in children with focal cortical dysplasia.

Methods

Seven pediatric patients diagnosed with focal cortical dysplasia by imaging were enrolled for this pilot study. The authors analyzed brain perfusion obtained by MRI in 2 of the children and brain tissue specimens obtained by epilepsy surgery on all of the children. An institutional review board approved this study, and parental consent was obtained.

Details of the selection process are as follows. Over the course of 1 year, 2 of the investigators tested the clinical value of using arterial spin labeling for the first MRI scan of all the infants less than 6 months of age and provided the following results to the remaining team of investigators. For this pilot study, the multidisciplinary team of investigators chose to review the imaging and histology of the patients (obtained over the course of the year) whose specimens were minimally distorted/fragmented or resected "en block". Further serial sectioning allowed them to measure the microvessel density in the area of focal cortical dysplasia and surrounding area.

Brain Imaging Analysis

Brain MRI scans were available for the 7 children with focal cortical dysplasia. In addition, the authors studied brain perfusion obtained by MRI and the perfusion imaging obtained by arterial spin labeling for 2 of the children. Blood flow measurements were performed in different brain regions of interest, including the area of focal cortical dysplasia. Focal cortical dysplasia was diagnosed by neuroradiologists using the conventional sequences.

Magnetic resonance imaging was performed using a 3-T Siemens Magnetom Trio (Siemens, Erlangen, Germany), a 32-channel head coil in most cases (Siemens),⁷ or a standard 12-channel head coil. A pulsed arterial spin labeling sequence (PICORE Q2TIPS)⁸ was acquired together with high spatial resolution anatomic T1- and T2-weighted images, diffusion-weighted images, and spectroscopy. Regional cerebral blood flow maps were obtained using the Siemens ASL Postprocessing Functor (Siemens). Quantitative estimates of regional cerebral blood flow were made using previously described formulas⁹ and parameters.¹⁰ Quantification of regional cerebral blood flow was performed using the cerebral blood flow maps. Manually drawn regions of interest were placed bilaterally in 4 types of tissue: cortical gray matter, white matter, basal ganglia, and within the area of focal cortical dysplasia, its edges, and symmetrically on the contralateral side. Measurements were obtained from the right and left sides of the cerebrum in several places for each of these 4 tissue regions to include the variations of perfusion in these areas. Regions of interest were drawn by a single investigator,

who was blinded to each patient's characteristics and outcome. For representation and statistical analysis, the ratio of cerebral blood flow ipsilateral to the lesions versus the contralateral side was determined to draw comparisons between the patients of different ages and to eliminate the age-related variation of the cerebral blood flow.

Histopathological Analysis

The authors analyzed the brain tissue specimens obtained from the epilepsy surgery on the 7 children with focal cortical dysplasia. In each case, focal cortical dysplasia was classified according to the Palmini classification¹ and the International League Against Epilepsy classification,² using hematoxylin and eosin staining, Klüver-Barrera staining, and Bielschowsky staining.

Immunohistochemistry. There were 5- μ m tissue sections of formalin-fixed, paraffin-embedded tissue used for immunohistochemical staining with a monoclonal mouse anti-human CD34 antibody (M7165, DAKO, Carpinteria, CA) (dilution, 1:400; incubation time, 1 hour at room temperature)¹¹ and a monoclonal mouse anti-human antiphosphorylated neurofilament antibody (SMI-31R, Covance, Emeryville, CA) (dilution, 1:5000; incubation time, 1 hour at room temperature).¹² The reaction was carried out in an automated immunohistochemistry instrument (DAKO). Antigen-antibody reactions were revealed with standardized development times using the DAKO Envision System.

Microvessel quantitation. Microvessel quantitation was performed by light microscopy by observers without previous knowledge of the tissue data. One to 3 fields of the highest microvessel count were assessed as previously described,^{13,14} and the result was expressed as a mean value. Briefly, the area of highest microvascular density was selected by scanning at 40 \times magnification. Then, the fields of the highest microvessels at 200 \times magnification were counted (0.785 mm² per field). Any CD34-positive endothelial cells, clearly separated from adjacent neuronal and glial cells, were considered to be a single countable microvessel. Branching structures were counted as a single vessel unless a break occurred in the continuity of the structure. The presence of either a lumen or erythrocyte in the lumen was not required to classify a structure as a vessel. Fragmented staining was not counted as a microvessel because it could represent the fragments of endothelial cells or the edges of dysplastic neurons. Three different areas were used for the measurements: (1) the area of focal cortical dysplasia containing dysplastic neurons; (2) the area "adjacent to focal cortical dysplasia," defined as the nearby cortical region that did not contain any abnormal cortical lamination and/or dysmorphic cells in close proximity to focal cortical dysplasia (ie, < 0.1 cm from the area containing dysplastic neurons); and (3) the area "surrounding focal cortical dysplasia," defined as the cortical area without morphological abnormalities estimated to be situated at least \geq 1 cm away from the area containing dysplastic neurons. One investigator took pictures of the respective fields of view at 200 \times magnification for each case and each area, 2 investigators assessed the microvessel count on each picture, and the average value of these 2 counts was determined. For comparison, the authors also calculated the microvessel count of 5 age-matched control tissues obtained from the autopsy material of children without focal cortical dysplasia or epilepsy.

Statistical Analysis

The outcomes of interest in this study were the cerebral blood flow measured by MRI and the microvessel count measured by

Table 1. Clinical Characteristics of the Study Patients.

	Patient 1	Patient 2	Patient 3	Patient 4	Patient 5	Patient 6	Patient 7	Control 1	Control 2	Control 3	Control 4	Control 5
Sex	Female	Male	Male	Female	Female	Male	Female	Female	Male	Male	Female	Male
Type of focal cortical dysplasia	I/A	I/A	I/A	I/B	I/B	I/B	I/B					
Location of focal cortical dysplasia	Right temporal	Left temporal	Right temporal	Right frontal	Left temporal	Right frontal	Right frontal					
Location of examined brain tissue (control children)	Right temporal	Left temporal	Right temporal	Right frontal	Left temporal	Right frontal	Right frontal	Left temporal	Right temporal	Right temporal	Right frontal	Left frontal
Reason for death (control children)								Brain bank: enterocolitis	Brain bank: sudden death/arrhythmia	Brain bank: sudden death/arrhythmia	Brain bank: accident	Brain bank: sudden death/arrhythmia
Age at surgery	3.5 mo	4.5 mo	13 y	6 mo	4 y	11 y	15 y	1 mo	9 mo	4 y	14 y	18 y
Microvessel count, mean	91.0	72.0	132.0	80.0	64.0	78.7	59.5	—	—	—	—	—
Area of focal cortical dysplasia	124.0	69.0	121.5	89.0	73.0	71.0	59.0	—	—	—	—	—
Adjacent area	60.5	30.0	63.3	39.0	36.0	34.0	31.0	24.7	27.0	34.0	39.7	46.3
Surrounding area	2.5 mo	—	—	21 d	—	—	—	—	—	—	—	—
Age at perfusion by magnetic resonance imaging	—	—	—	—	—	—	—	—	—	—	—	—
Cerebral blood flow, mean	1.95	—	—	1.98	—	—	—	—	—	—	—	—
Ratio of focal cortical dysplasia, ipsilateral/contralateral	1.00	—	—	1.01	—	—	—	—	—	—	—	—
Ratio of cortical gray matter, ipsilateral/contralateral	0.97	—	—	0.92	—	—	—	—	—	—	—	—
Ratio of white matter, ipsilateral/contralateral	1.01	—	—	1.02	—	—	—	—	—	—	—	—
Ratio of basal ganglia, ipsilateral/contralateral	—	—	—	—	—	—	—	—	—	—	—	—

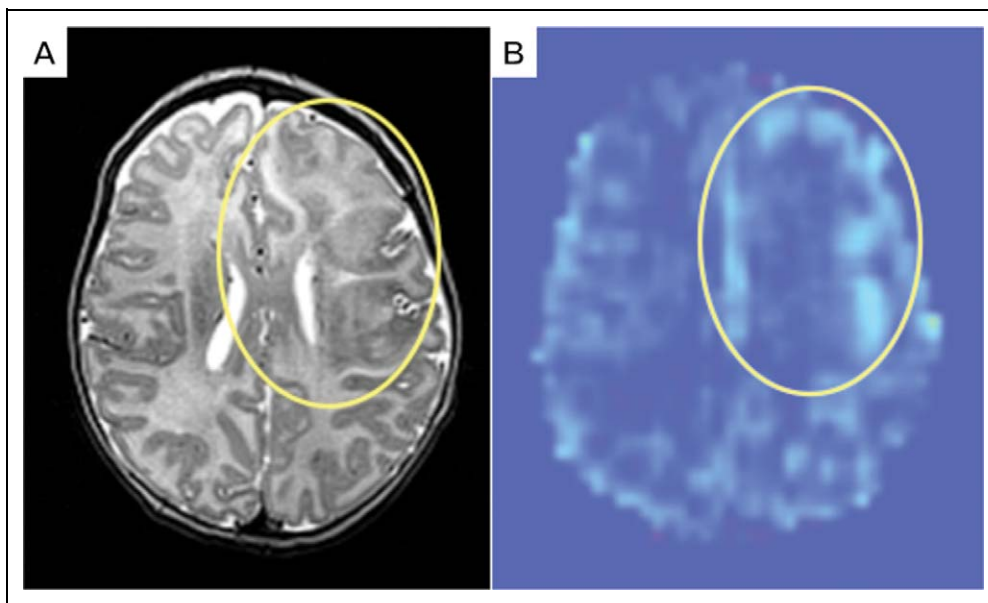


Figure 1. Brain magnetic resonance imaging on day 21 of life in a patient with focal cortical dysplasia: comparison between T2-weighted images and perfusion map. (A) T2-weighted imaging showing disorganization of the normal structure of the cerebral cortex within the left frontal lobe (within oval). (B) Perfusion map showing increased brain perfusion in the area of focal cortical dysplasia (within oval) compared to the contralateral side. Of note, the patient did not present clinical seizures during the brain magnetic resonance imaging.

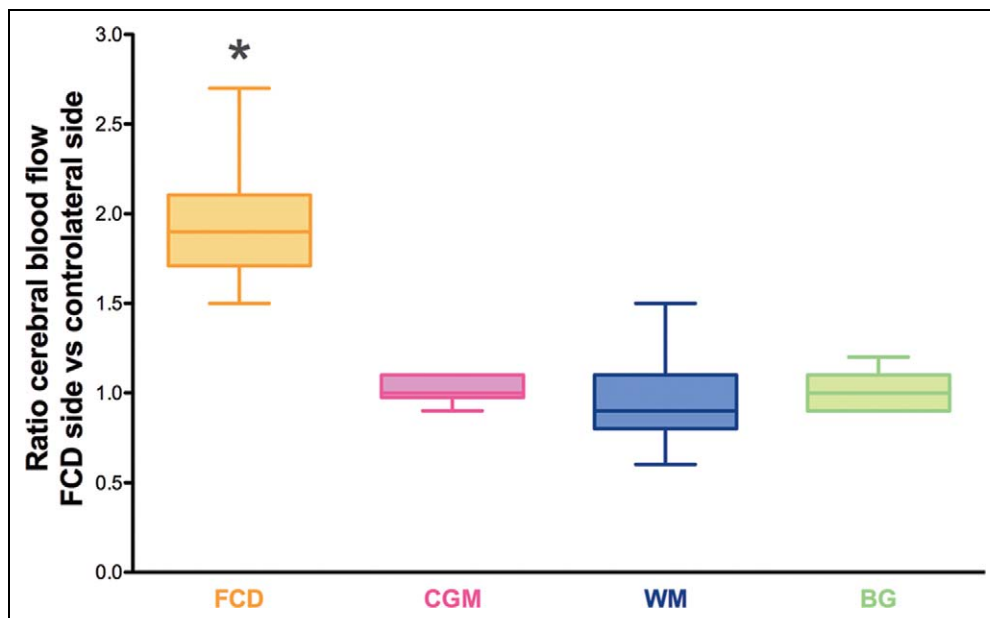


Figure 2. Ratio of cerebral blood flow values in each region of interest (ipsilateral to the lesion vs contralateral) in 2 children with focal cortical dysplasia. Box and whisker plots (median, minimum, and maximum). The different regions of interest consist of the (1) area of focal cortical dysplasia (FCD) versus symmetric contralateral area; (2) remaining cortical gray matter (CGM), including frontal, parietal, and occipital cortical regions; (3) remaining white matter (WM), including frontal and posterior white matter and centrum semiovale; and (4) basal ganglia (BG), including thalamus, lentiform nucleus, and posterior limb of internal capsule. The ratio of cerebral blood flow was significantly increased within the area of focal cortical dysplasia compared to the remaining parts of the brain (* $P < .0001$).

histopathology. For each outcome, the authors calculated the means and standard errors. To assess the differences in the ratio of cerebral blood flow or the microvessel counts, they performed statistical analyses using the Student *t* test. A *P* value $< .05$ was considered significant.

Results

For the experiments described in this present study, the authors used the brain MRI scans of 7 children with focal cortical dysplasia (perfusion imaging by arterial spin labeling was only available for 2 of these

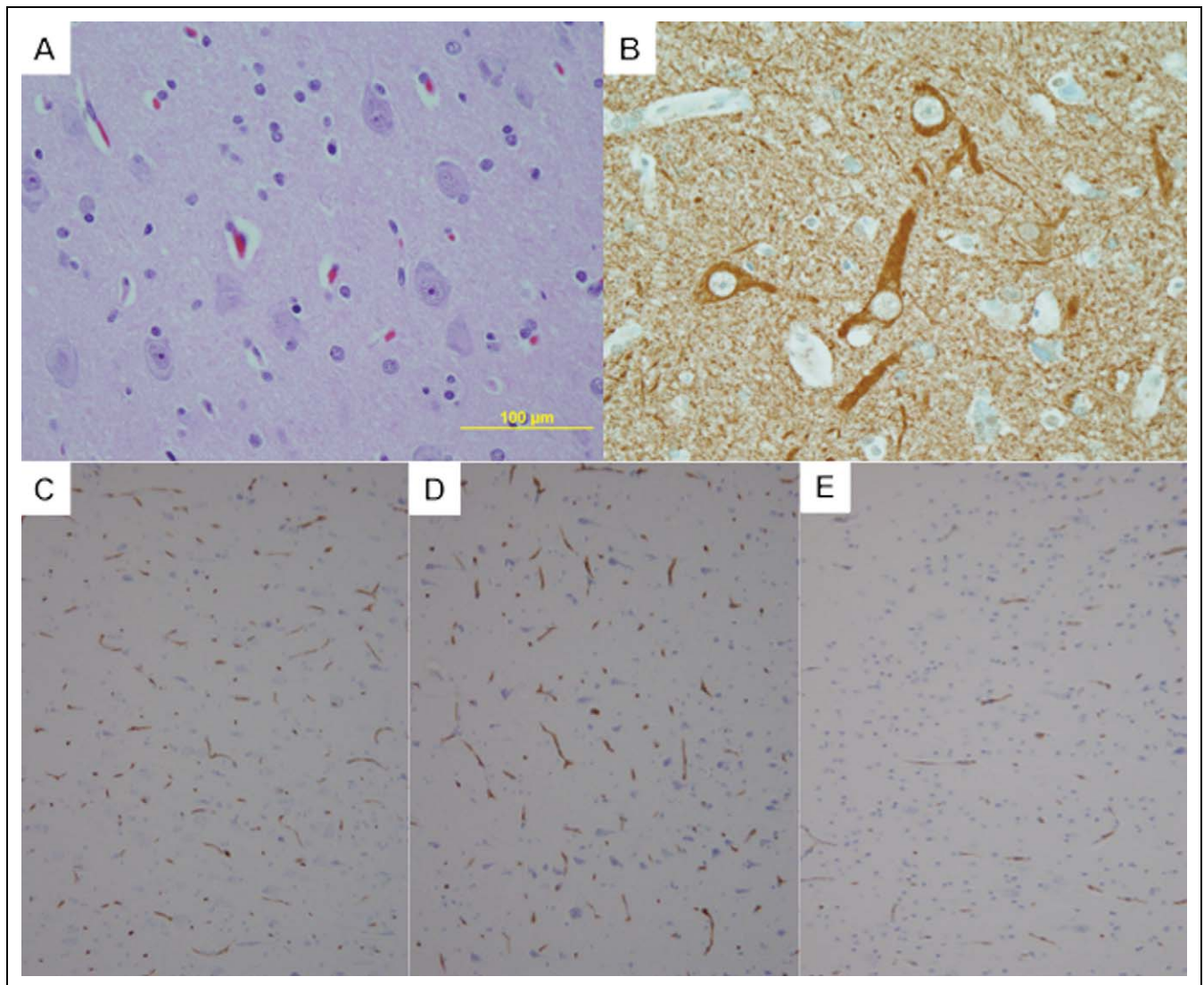


Figure 3. Microscopic features of focal cortical dysplasia type IIa. (A) Hematoxylin and eosin staining shows architectural abnormalities with dysmorphic neurons but without balloon cells (400 \times). (B) Abnormal accumulation of phosphorylated neurofilaments (SMI-31) is observed in the perikaryon of dysmorphic neurons (400 \times). (C-E) CD34 immunohistochemical evaluation demonstrating numerous microvessels in the area of focal cortical dysplasia (C) and in the adjacent area (D) compared to the surrounding cortex without morphological abnormalities (E) (200 \times).

patients) and the brain tissue specimens obtained from epilepsy surgery on these same children (Table 1). The age at surgery ranged from 3 months to 14 years. The gender of the children included 3 males and 4 females.

Brain Imaging Analysis

Focal cortical dysplasia was diagnosed on the conventional sequences of these 7 children. Perfusion imaging was obtained only for 2 of the children. The first patient (Figure 1) was 21 days old at the time of her first MRI scan and perfusion imaging scan; she was later operated on at 6 months of age for refractory seizures, and she was diagnosed with focal cortical dysplasia type IIB. The second patient was 4 months old at the time of her first MRI scan and perfusion imaging scan; she was later operated on at 5 months of age for refractory seizures, and she was diagnosed with focal cortical dysplasia type IIA. Both patients underwent their initial MRI scan and thus the perfusion scan for

seizure activity, but neither presented with clinically evident seizures at the time of brain MRI. In addition, the electroencephalogram was within normal limits on the same day as the imaging was performed on these 2 patients.

Both patients presented different values of cerebral blood flow throughout the cerebral hemispheres. Cerebral blood flow was 33.8 ± 0.4 and 89.3 ± 3.2 mL/100 g/min in the cortical gray matter, 3.3 ± 0.2 and 10.1 ± 1.0 mL/100 g/min in the white matter, and 23.5 ± 0.6 and 54.1 ± 2.9 mL/100 g/min in the basal ganglia, respectively, for each of these 2 patients. However, to draw comparisons between the 2 patients and remove the age-related variation of cerebral blood flow, the ratio of cerebral blood flow ipsilateral to the lesions versus the contralateral side was calculated. Cerebral blood flow within the area of focal cortical dysplasia and adjacent regions was approximately double in both patients compared to the contralateral side (ratio of ipsilateral vs contralateral side: 1.98 ± 0.07 and 1.95 ± 0.09 within the area of focal cortical dysplasia, respectively, in each of these 2 patients) (Table 1 and Figure 2). In

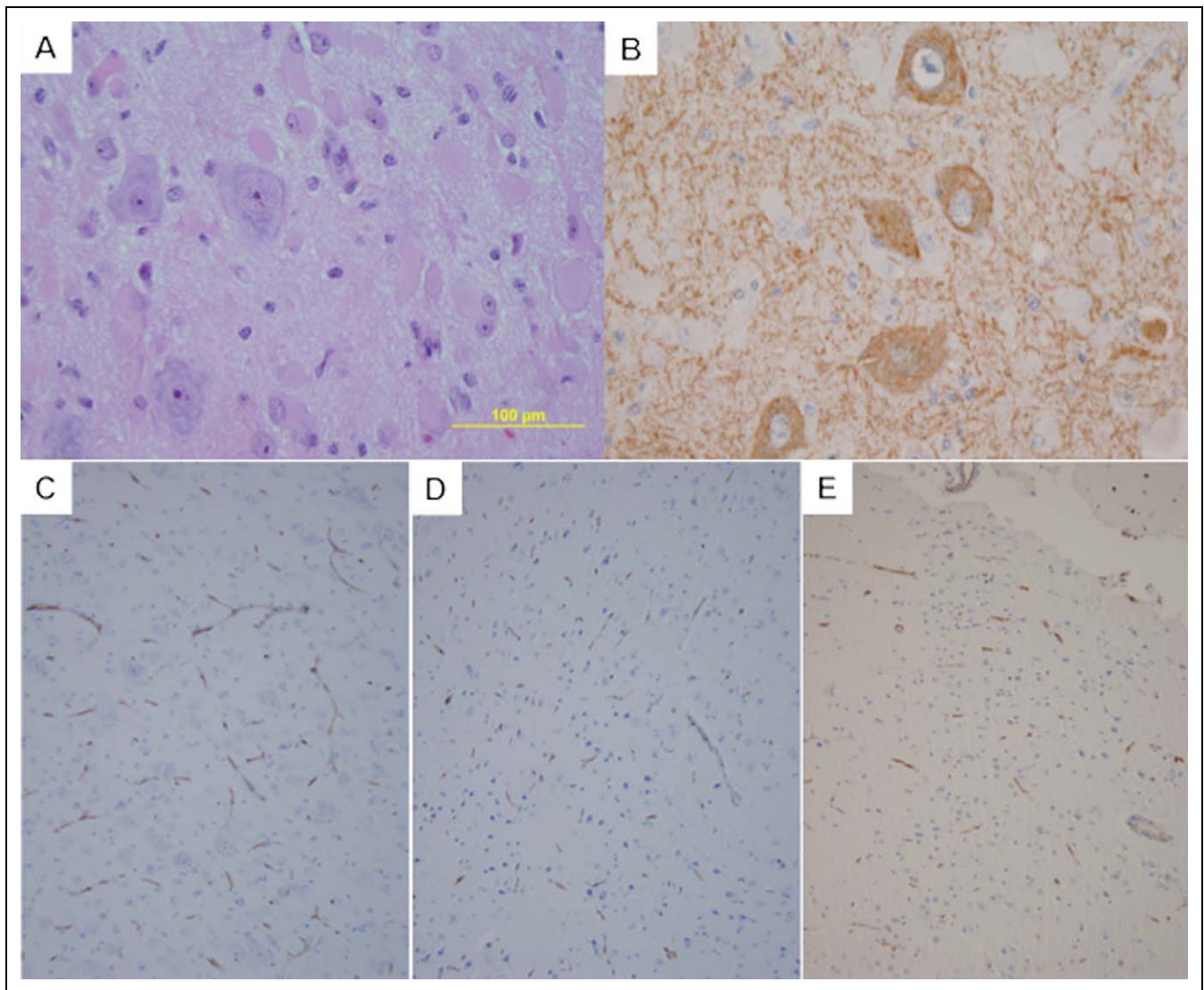


Figure 4. Microscopic features of focal cortical dysplasia type IIb. (A) Hematoxylin and eosin staining shows architectural abnormalities with dysmorphic neurons and balloon cells (400 \times). (B) Abnormal perikaryon expression of phosphorylated neurofilament (SMI-31) in dysplastic neurons (400 \times). (C-E) CD34 immunohistochemical evaluation demonstrating numerous microvessels in the area of focal cortical dysplasia (C) and in the adjacent area (D) compared to the surrounding cortex without morphological abnormalities (E) (200 \times).

the remaining morphologically normal parts of the brain, cerebral blood flow was comparable from one side to the other (ratio of ipsilateral vs contralateral brain side: 0.99 ± 0.03 and 0.99 ± 0.02 in the remaining brain, respectively, in each of these 2 patients) (Table 1 and Figure 2). Statistical analysis revealed the differences in the ratio of cerebral blood flow to be significantly increased within the area of focal cortical dysplasia compared to the remaining parts of the brain ($P < .0001$). Although the authors recognize the limitations of running a statistical analysis on data obtained for only 2 patients, nonetheless, they decided to present these results due to the highly different values yielded by the analysis.

Histopathological Analysis

Morphological changes were analyzed for a total of 7 children with pharmacoresistant epilepsy. Three patients were classified with focal cortical dysplasia type IIa (Figure 3) and 4 patients with focal cortical

dysplasia type IIb (Figure 4) by both the Palmini classification and the International League Against Epilepsy classification.

Areas of focal cortical dysplasia showed abnormal cortical lamination and dysplastic neurons randomly arranged through layers II to VI. An abnormal perikaryon expression of the phosphorylated neurofilament (SMI-31) was noted in the immunohistochemical evaluation of dysplastic neurons. Areas adjacent to or surrounding focal cortical dysplasia were defined as nearby cortical regions that did not contain any abnormal cortical lamination and/or dysmorphic cells, either situated < 0.1 cm from the area containing dysplastic neurons (“adjacent” area) or at least ≥ 1 cm away from the area containing dysplastic neurons (“surrounding” area).

The mean microvessel count per 200 \times field yielded was 82.5 ± 9.2 in the area of focal cortical dysplasia and 86.6 ± 9.9 in the adjacent area ($P = .48$; no statistical difference) (Table 1 and Figure 5). On the other hand, the corresponding value yielded in the surrounding area was

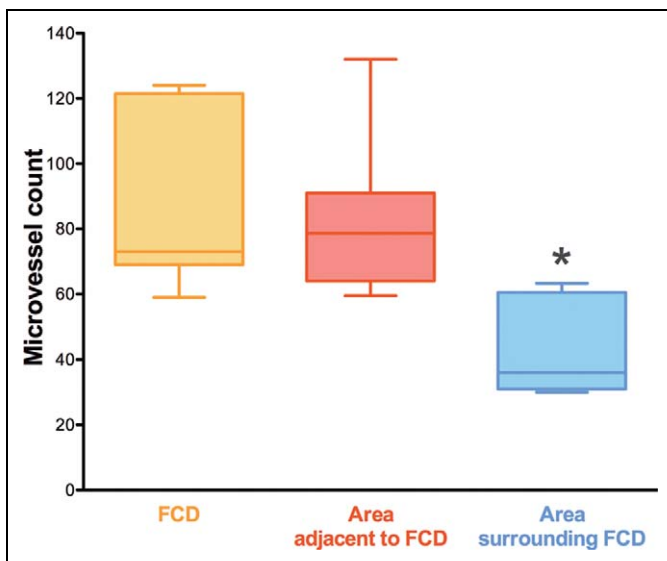


Figure 5. Microvessel count in 7 children with focal cortical dysplasia. Box and whisker plots (median, minimum, and maximum). The different regions of interest consist of the (1) area of focal cortical dysplasia (FCD), (2) area adjacent to focal cortical dysplasia, and (3) area surrounding focal cortical dysplasia. The area adjacent to focal cortical dysplasia was as highly vascularized as the area of focal cortical dysplasia ($P = \text{not significant}$). The microvessel count in the area surrounding focal cortical dysplasia was almost 2 times lower ($*P = .0003$) than the microvessel count recorded within the area of focal cortical dysplasia and at its edges.

almost 2 times lower (42.0 ± 5.3) and statistically significantly lower ($P = .0003$) than the microvessel count recorded within the area of focal cortical dysplasia and at its edges (Table 1 and Figure 5).

By distinguishing the patients according to their respective subgroup of focal cortical dysplasia, the authors found the same ratio difference. With respect to focal cortical dysplasia type IIa, the mean microvessel count per $200\times$ field was 98.3 ± 17.7 in the area of focal cortical dysplasia, 104.8 ± 17.9 in the adjacent area, and 51.3 ± 10.7 in the surrounding area. With respect to focal cortical dysplasia type IIb, the mean microvessel count per $200\times$ field was 70.5 ± 3.9 in the area of focal cortical dysplasia, 73.0 ± 4.7 in the adjacent area, and 35.0 ± 1.3 in the surrounding area. The microvessel count in each respective area seemed to be higher ($P \leq .05$) in children with focal cortical dysplasia type IIa compared to children with focal cortical dysplasia type IIb. Again, the authors recognize the limitation of running a statistical analysis and drawing conclusions on so few patients.

For comparison, the mean microvessel count per $200\times$ field in the same brain areas was 34.3 ± 8.9 in age-matched control tissues obtained from autopsy material of children without focal cortical dysplasia or epilepsy. This result was similar ($P = .31$) to the microvessel count of the area surrounding focal cortical dysplasia obtained from the 7 children with focal cortical dysplasia.

Discussion

Classically, hyperperfusion in cases of focal cortical dysplasia has been attributed to functional alterations due to seizure activity. However, the novel findings of the present study indicate that the hyperperfusion observed on imaging highly correlates with the increased microvessel density observed in the morphological studies of patients with focal

cortical dysplasia type IIa and IIb (ie, brain perfusion was approximately 2 times higher in the area of focal cortical dysplasia compared to the contralateral side, and the microvessel density was nearly double in the area of focal cortical dysplasia compared to the surrounding cortex that did not have morphological abnormalities). Interestingly, the area adjacent to focal cortical dysplasia, although not containing morphological findings of focal cortical dysplasia (architectural abnormalities, dysplastic neurons, and balloon cells), was as highly vascularized as the area of focal cortical dysplasia. At this point, the authors cannot resolve whether abnormal neuronal migration is causing an abnormal development and increased numbers of vessels in the area of focal cortical dysplasia or conversely whether abnormal blood vessel development has led to the development of focal cortical dysplasia. It is known that prenatal vasculogenesis is required to support normal neuronal migration and maturation; an alteration of this process leads to the failure of normal cerebrovascular development and can have profound implications for central nervous system maturation.⁵ Also, additional studies are warranted for patients with focal cortical dysplasia type Ia and Ib, cortical tubers, and other malformations of cortical development to determine if other forms of cortical maldevelopment can have similar findings.

The current understanding is that seizures cause local hypermetabolism and thus hyperperfusion in focal cortical dysplasia. Another possibility raised by the present findings is that the hyperperfusion in focal cortical dysplasia, which correlates with an increase in the number of microvessels in the area affected by focal cortical dysplasia, might thus be a contributing factor to, rather than a consequence of, seizures. Evidence is lacking that seizures cause the growth of additional microvessels, especially since 1 of the patients displayed hyperperfusion shortly after birth before presenting with seizures (ie, no clinical seizures before MRI and normal electroencephalogram finding on the same day as MRI). It also is unlikely that the antiepileptic treatment has caused the growth of these additional microvessels because the same patient only received antiepileptic medication long after her brain imaging. The pathogenesis of seizures in cases of focal cortical dysplasia might be caused by hypermetabolism due to an increased perfusion of the area. These findings warrant further investigation using animal models to determine the relationship between brain perfusion, microvascular density, and seizure activity in focal cortical dysplasia.

From a clinical point of view, as demonstrated with other brain diseases,¹⁵ to better delineate focal cortical dysplasia and other malformations of cortical development prior to epilepsy surgery, perfusion imaging by MRI might provide a useful addition to other MRI sequences and to single-photon emission computed tomography and positron emission tomography. One current limitation of today's epilepsy surgery for focal cortical dysplasia is the difficulty in exactly defining the extent of focal cortical dysplasia on MRI, which often leads to only a partial resection and lack of control of the seizure activity. Thus, developing additional tools to assist in this area is thus of utmost importance to improve the treatment of these patients. Perfusion imaging by MRI has indicated an increased perfusion in the area of focal cortical dysplasia and its vicinity, which correlates with an increased vessel count. This result can reflect a larger epileptogenic network beyond the extent of focal cortical dysplasia seen in the conventional MRI sequences and even beyond the histological areas of abnormal cellular organization. For better control of the seizures, this information also can provide a basis for why surgical removal should include not only the area of focal cortical dysplasia but potentially also the adjacent region.

The main limitation of this pilot study is the small number of patients. However, to the authors' knowledge, this study is the only such

study that measures brain perfusion obtained by MRI in children with focal cortical dysplasia and that correlates this perfusion with a histopathological analysis. Absolute measurements by perfusion imaging with arterial spin labeling, despite their known limitations,^{9,16} permit the noninvasive assessment of perfusion in different regions of interest of children's brains and a comparison among these children. The current results in children with focal cortical dysplasia show the feasibility of using the arterial spin labeling method and support the addition of perfusion imaging by arterial spin labeling to the current imaging sequences performed on these patients, as well as the addition of histopathological correlation for the surgical cases, to definitively prove the authors' hypothesis in a larger number of patients. Another limitation of this pilot study is the wide range of the children's ages at the time of MRI and/or surgery. As such, both patients presented different values of cerebral blood flow throughout the cerebral hemispheres; this phenomenon is known to be related to their age difference at the time of the perfusion imaging scan. However, to draw comparisons between the 2 patients and remove the age-related variation of cerebral blood flow, the ratio of cerebral blood flow ipsilateral to the lesions versus the contralateral side was calculated. A third limitation is that CD34 labels endothelial cells but also some dysplastic neurons; however, the morphologies of these 2 types of cells are different, which permits the exclusion of the dysplastic neurons in the microvessel count. Fragmented staining was not counted as a microvessel because they could represent the fragments of endothelial cells or the edges of dysplastic neurons.

In conclusion, perfusion anomalies of focal cortical dysplasia cannot necessarily be related to epileptic activity; rather, these anomalies can be related to blood vessel alterations. Perfusion imaging by MRI is a useful way to demonstrate these abnormalities in cerebral microvessels. Further imaging and histopathological studies are needed to more accurately determine the relationship between perfusion, microvascular density, and epileptogenesis in cases of focal cortical dysplasia.

Acknowledgments

The authors are thankful to Mei Zheng, HTL (ASCP), QIHC, clinical supervisor of the Immunohistochemical Laboratory in the Department of Pathology and the DF/HCC Pathology Core at Brigham and Women's Hospital, Boston, for their excellent help with the immunohistochemical studies.

Author Contributions

This article has been read and approved by all the authors. PW and ML contributed equally to this article; they collected the data, analyzed the results, and wrote the article. BK brought his expertise to the histopathological analysis, critically revised the article, and approved the final version. SKW and FEJ supervised the work of PW and ML (the imaging analysis and the histopathological analysis, respectively); they critically revised the article and approved the final version. MT, AP, and AMB enrolled the patients in the study and obtained consent; they critically revised the article and approved the final version. JRM operated on all the patients and provided the brain samples; he critically revised the article and approved the final version. SW helped to obtain the imaging scans; he critically revised the article and approved the final version. All the authors fulfill the authorship credit requirements.

Declaration of Conflicting Interests

The authors declared no potential conflicts of interest with respect to the research, authorship, and/or publication of this article.

Funding

The authors disclosed receipt of the following financial support for the research, authorship and/or publication of this article: This work was supported by the William Randolph Hearst Fund Award (to PW) and the Thrasher Research Fund Early Career Award Program (to PW). SKW is supported by National Institutes of Health grants R01 RR021885, R01EB008015, and R01 LM010033. AP is supported by the National Institute of Neurological Disorders and Stroke (K23NS069784). FEJ is supported by NIH R01 NS 031718 and NIH DP1 GMS OD003347.

Ethical Approval

An institutional review board approved this study, and parental consent was obtained.

References

1. Palmi A, Najm I, Avanzini G, et al. Terminology and classification of the cortical dysplasias. *Neurology*. 2004;62(6 Suppl 3): S2-S8.
2. Blumcke I, Thom M, Aronica E, et al. The clinicopathologic spectrum of focal cortical dysplasias: a consensus classification proposed by an ad hoc task force of the ILAE Diagnostic Methods Commission. *Epilepsia*. 2011;52(1):158-174.
3. Arbiser JL, Flynn E, Barnhill RL. Analysis of vascularity of human neurofibromas. *J Am Acad Dermatol*. 1998;38(6 Pt 1): 950-954.
4. Hamilton SJ, Friedman JM. Insights into the pathogenesis of neurofibromatosis 1 vasculopathy. *Clin Genet*. 2000;58(5):341-344.
5. Hallene KL, Oby E, Lee BJ, et al. Prenatal exposure to thalidomide, altered vasculogenesis, and CNS malformations. *Neuroscience*. 2006;142(1):267-283.
6. Wintermark P, Roulet-Perez E, Maeder-Ingvar M, et al. Perfusion abnormalities in hemimegalencephaly. *Neuropediatrics*. 2009; 40(2):92-96.
7. Wiggins GC, Triantafyllou C, Potthast A, et al. 32-channel 3 Tesla receive-only phased-array head coil with soccer-ball element geometry. *Magn Reson Med*. 2006;56(1):216-223.
8. Luh WM, Wong EC, Bandettini PA, et al. QUIPSS II with thin-slice T1 periodic saturation: a method for improving accuracy of quantitative perfusion imaging using pulsed arterial spin labeling. *Magn Reson Med*. 1999;41(6):1246-1254.
9. Wang J, Licht DJ, Jahng GH, et al. Pediatric perfusion imaging using pulsed arterial spin labeling. *J Magn Reson Imaging*. 2003;18(4):404-413.
10. Cavuşoğlu M, Pfeuffer J, Uğurbil K, et al. Comparison of pulsed arterial spin labeling encoding schemes and absolute perfusion quantification. *Magn Reson Imaging*. 2009;27(8):1039-1045.
11. Fina L, Molgaard HV, Robertson D, et al. Expression of the CD34 gene in vascular endothelial cells. *Blood*. 1990;75(12): 2417-2426.
12. Raina AK, Takeda A, Nunomura A, et al. Genetic evidence for oxidative stress in Alzheimer's disease. *Neuroreport*. 1999;10:1.
13. Weidner N, Semple JP, Welch WR, et al. Tumor angiogenesis and metastasis: correlation in invasive breast carcinoma. *N Engl J Med*. 1991;324(1):1-8.

14. Ogawa Y, Chung YS, Nakata B, et al. Microvessel quantitation in invasive breast cancer by staining for factor VIII-related antigen. *Br J Cancer*. 1995;71(6):1297-1301.
15. Noguchi T, Yoshiura T, Hiwatashi A, et al. Perfusion imaging of brain tumors using arterial spin-labeling: correlation with histopathologic vascular density. *AJNR Am J Neuroradiol*. 2008;29(4):688-693.
16. Zappe AC, Reichold J, Burger C, et al. Quantification of cerebral blood flow in nonhuman primates using arterial spin labeling and a two-compartment model. *Magn Reson Imaging*. 2007;25(6):775-783.